SSRG International Journal of Electrical and Electronics Engineering
ISSN: 2348-8379/ https://doi.org/10.14445/23488379/IJEEE-V11I6P122

Volume 11 Issue 6, 197-204, June 2024
© 2024 Seventh Sense Research Group®

Original Article

Novel Multi-Stage Hybrid-Smart Load-Frequency Controller to an Interconnected Power System Considering HVDC and Renewable Energy Sources

Diem-Vuong Doan[1], Ngoc-Khoat Nguyen[1*]

[1]*Faculty of Control and Automation, Electric Power University, Hanoi, Vietnam.*

**Corresponding Author : khoatnn@epu.edu.vn*

Received: 10 April 2024 Revised: 13 May 2024 Accepted: 10 June 2024 Published: 29 June 2024

Abstract *- Large-scale power systems constitute interconnected networks comprising numerous highly complex devices, presenting a significant challenge for control strategies. Within such systems, maintaining stable frequency control across regions remains one of the most pressing issues today. This study proposes a novel design for a multi-stage hybrid controller applicable to a complex two-area interconnected power system. Each area in this system incorporates three distinct turbine types. The controller integrates a PID controller with a (2+PI) controller structure, further augmented by a fuzzy logic component. The parameters of this multi-stage PID-(2+PI) controller are optimized using a modified, faster variant of Particle Swarm Optimization (iPSO). The frequency response of the two areas, obtained through simulations conducted using the MATLAB/Simulink software package, is compared with the performance of PSO-PID and conventional PID controllers. These comparisons with a lot of numerical simulations demonstrate that the proposed controller yields significantly superior results, thereby validating the feasibility of this control approach.*

Keywords *- iPSO, Fuzzy logic, PID, (2+PI), Multi-stage controller, Interconnected power system, LFC.*

1. Introduction

The growing global demand for electricity drives the interconnection of an increasing number of diverse generation units via existing transmission lines (tie-lines). This increasing system complexity, scale, and vulnerability to unanticipated internal and external disturbances present a significant challenge for Power System (PS) engineering, especially concerning the design of robust control systems. A fundamental principle in maintaining PS stability and distribution is ensuring that the active power output from generators precisely matches the system's power demand while minimizing transmission losses. This control strategy can be referred to as Load-Frequency Control (LFC).

Essentially, LFC enables synchronous generators to dynamically adjust their power output in response to fluctuating load demands. This ensures that any deviations in power and frequency within a specific area, as well as tie-line power flow errors, converge to zero. However, inadequate LFC design can result in performance degradation, characterized by significant and unexpected errors. Moreover, oscillations in generation, area and line frequencies and currents can destabilize the system, leading to synchronization loss. In light of these factors above, the formulation of sophisticated and efficacious control methodologies emerges as an indispensable prerequisite for guaranteeing robust LFC within Power Systems (PSs).

The comprehensive literature review indicates a wealth of highly valuable information that has surfaced, referencing research efforts in the realm of LFC over the past decade. Each contribution aims to advance the field more sequentially and effectively compared to its predecessors. Recent research endeavors have employed various approaches, including the utilization of a PI/PID controller structure with algorithms such as BFOA [1] and hBFOA-PSO (an integration of the BFOA and the PSO) [2], the Firefly Algorithm (FA) [3] for optimizing PI controllers, a chaotic algorithm based on the Lozi map [4], the GA combined with DE [5], Ant Colony Optimization (ACO) [6], and ISFS, which has been known as an improved stochastic fractal search mechanism [7].

The integration of Renewable Energy Sources (RES) into contemporary power systems, while widely popular due to its environmental benefits, presents a number of technical challenges. These challenges stem from the inherent variability and intermittency of RES, which contributes to increased system nonlinearity. Furthermore, high penetration of RES can lead to a reduction in system inertia, a key factor in maintaining grid stability. Additionally, increased RES

This is an open access article under the CC BY-NC-ND license (http://creativecommons.org/licenses/by-nc-nd/4.0/)

integration can exacerbate frequency deviations within specific areas, elevate transmission line losses, and potentially reduce the operational capacity of existing electric power grid equipment.

Studies have explored various optimization techniques for power system control with renewable energy integration. Report [8] applies an adaptive model predictive controller, while [9] investigates a DEPSO hybrid controller for optimizing fuzzy PID parameters in a power system. Similarly, research in [10] focuses on PID parameter optimization through a combination of ANFIS and PSO methods. The study [11] addresses frequency stabilization in a power system with wind power by optimizing FOC using PSO.

Other studies, such as [12, 13], explore control parameter search for nonlinear power systems employing the cuckoo method, achieving frequency stabilization with electrical and solar power sources, respectively. Reference [14] optimizes PID parameters through the frequency-stabilized cuckoo method, and [15] proposes a method using BFOA for optimizing PID controller parameters in a system with renewable energy sources. These studies demonstrate the growing need for robust control strategies as power systems become increasingly complex with the integration of diverse renewable energy sources, particularly regarding frequency stability.

This article underwent further evaluation considering the influence of High Voltage Direct Current (HVDC) integration. HVDC links, operating concurrently with AC transmission lines, enhance power quality and bolster system resilience against minor disturbances. The proposed control strategy within the paper targets frequency regulation in two interconnected areas. Each region encompasses three turbine types: reheat, hydro, and gas. Notably, both areas incorporate HVDC and renewable energy sources.

The structure of this article is as follows. Section 2 details the design of a multi-stage PID+(2+PI) controller integrated with the fuzzy logic structure. Section 3 focuses on system modelling and simulation of the frequency error response in two interconnected areas under varying load shapes and magnitudes. Section 4 concludes the paper. The applicability of the methodology studied in this work is verified via numerical simulation results obtained using MATLAB/Simulink software.

2. Design of a PSO - PID - (2+PID) Structure with a Fuzzy Logic Controller

The control strategy leverages the Area Control Error (ACE) signal, defined in Equation (1), as the primary input. This aligns with the bias control principle, where the objective is to regulate the ACE signal to zero. By maintaining a zero ACE, the controller ensures that the net interchange of power between interconnected areas remains balanced. This, in turn, contributes to maintaining system frequency stability within acceptable tolerances.

$$ACE_i(t) = B_i \Delta f_i(t) + \Delta P_{tie}(t) \quad (1)$$

The working principle of the controller proposed in this study is given in Equation (2). Here, two stages, PID and (2+PI) regulators, are embedded in series to form the conventional control phase. The (2+PI) controller is modified from the (1+PI) regulator, which was introduced in [16].

$$\Delta P_{ref}(s) = \begin{bmatrix} ACE(s).\left(K_{P1} + \dfrac{K_{i1}}{s} + K_{d1}.s\right) \\ -\Delta f(s) - \Delta P_{tie}(s) \end{bmatrix}. \left(2 + K_{P2} + \frac{K_{i2}}{s}\right) \quad (2)$$

The PID-(2+PI) controller is then combined with the fuzzy logic controller based on the PI principle (PI–like FLC). Such a principle is shown in Figure 1, making the hybrid control methodology.

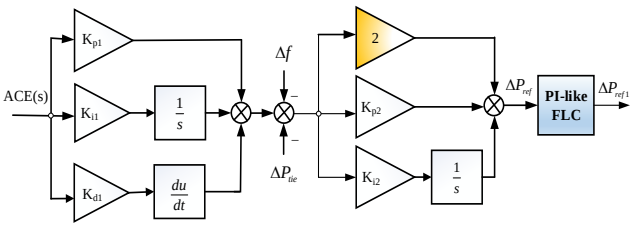

Fig. 1 Structure of PID-(2+PI) with PI-like fuzzy logic controller

The fuzzy controller, considered an intelligent control methodology, is designed with two inputs, ΔPref1, dΔPref1 and two outputs, Kp and Ki, which have the following membership functions shown in Figures 2, 3, 4 and 5.

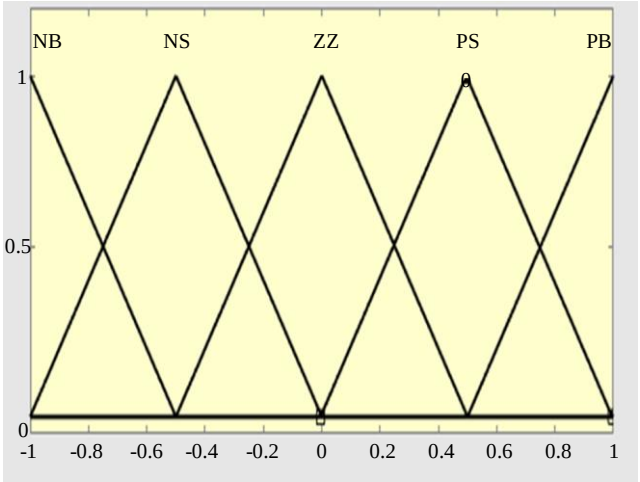

Fig. 2 The membership functions of ΔP_{ref1}

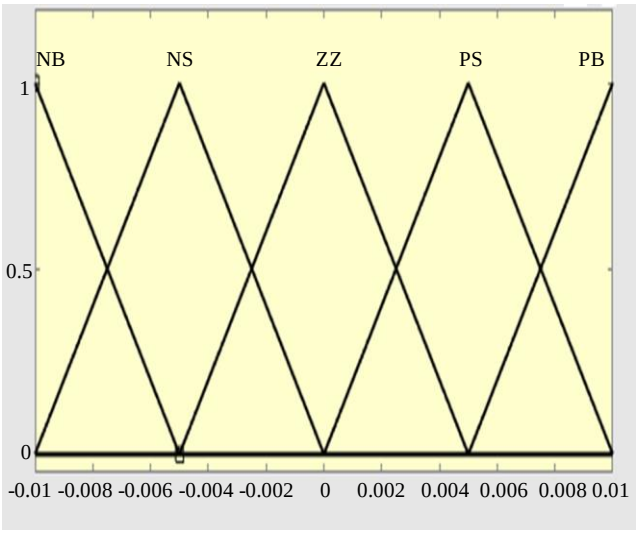

Fig. 3 The membership functions of $d\Delta P_{ref1}$

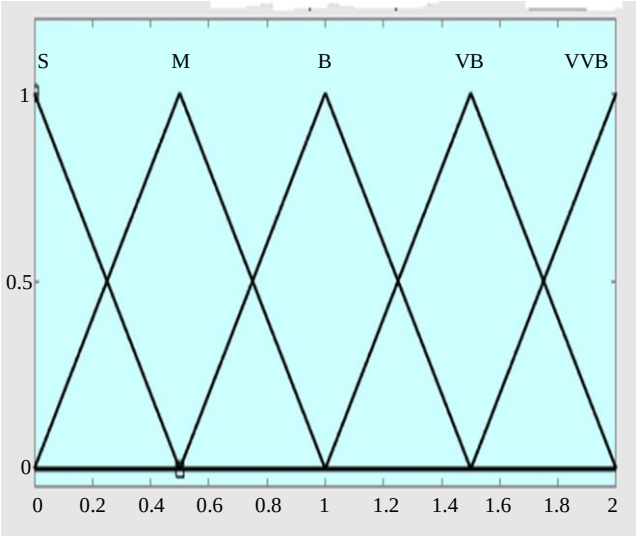

Fig. 4 The membership functions of K_p

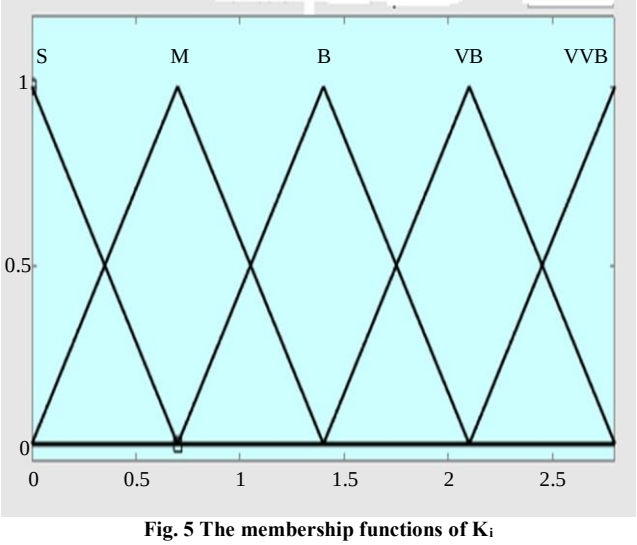

Fig. 5 The membership functions of K_i

The fuzzy logic rules for K_p and K_i corresponding to two outputs, K_p and K_i are illustrated in Tables 1 and 2.

Table 1. A set of fuzzy logic rules applied for K_p

ΔP_{ref1}						
$d\Delta P_{ref1}$		NB	NS	ZZ	PS	PB
	NB	S	S	M	M	B
	NS	S	M	M	B	VB
	ZZ	M	M	B	VB	VB
	PS	M	B	VB	VB	VVB
	PB	B	VB	VB	VVB	VVB

Table 2. An illustration of fuzzy logic rules for K_i

ΔPref1						
dΔPref1		NB	NS	ZZ	PS	PB
	NB	S	S	M	M	B
	NS	S	M	M	B	VB
	ZZ	M	M	B	VB	VB
	PS	M	B	VB	VB	VVB
	PB	B	VB	VB	VVB	VVB

This study employs an optimization technique to ascertain the optimal parameter set for the multi-stage PID-(2+PI) controller. A variant of the well-established Particle Swarm Optimization (PSO) mechanism, termed *i*PSO, is specifically chosen for this purpose. The PSO, inspired by the collective foraging behavior of bird or fish flocks, is recognized as one of the most efficacious optimization methods derived from biological principles. The algorithm commences by initializing a population of virtual 'particles' within the defined search space. During each iteration, these particles traverse the search space at designated velocities, aiming to locate the solution that optimizes the chosen objective function.

Particle velocity updates occur iteratively based on three factors: their current velocity, their individual best solution encountered so far (known as their 'pbest'), and the globally optimal solution discovered by the entire swarm to date (known as 'gbest'). These particles have positions which are iteratively re-computed based on the new velocities until a pre-defined termination criterion is met, signifying convergence.

To expedite convergence towards the global optimum, a modification is introduced to the conventional PSO. The optimization process leverages a very fast optimization mechanism as an initialization step. This demonstrably improves the likelihood of the swarm converging upon the optimal solution within the search space. A detailed illustration of the proposed *i*PSO mechanism is provided in Figure 6. Remember that the integration of an initial step using a fast optimization method is a new finding of this work.

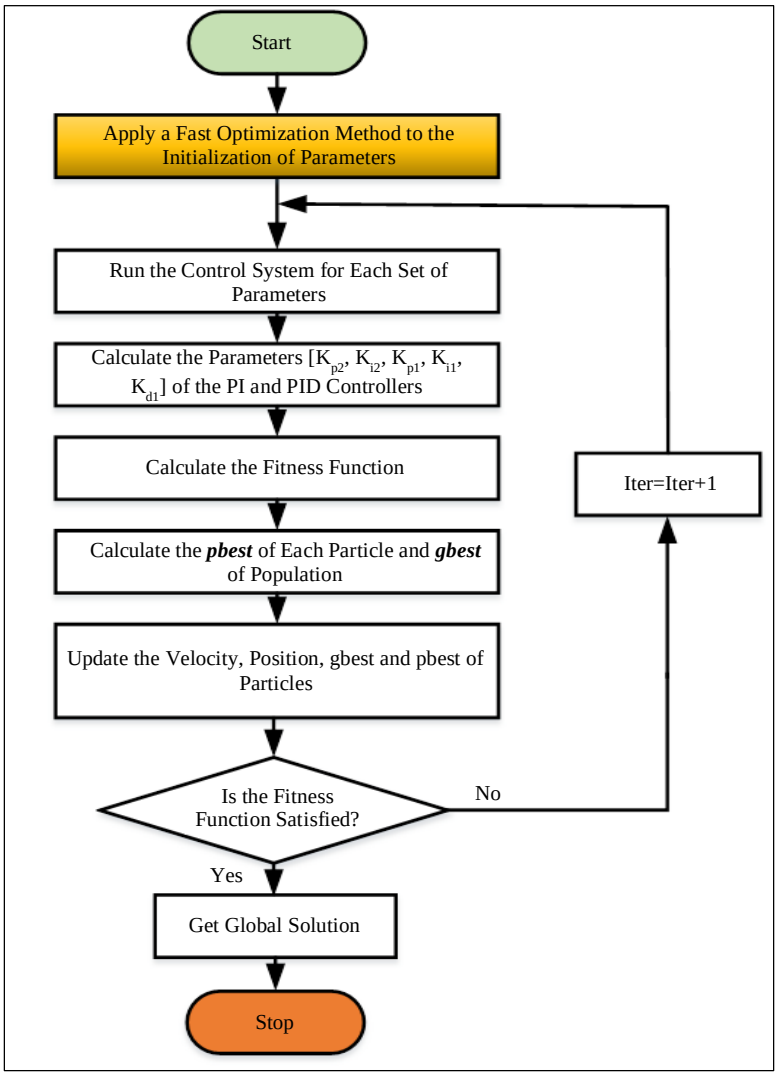

Fig. 6 The *i*PSO method to find an optimal set of parameters for the proposed regulator

The coefficients K_{p1}, K_{i1}, K_{d1}, K_{p2}, and K_{i2} are optimized by the *i*PSO method. The objective function or the fitness function used for such an *i*PSO method is expressed by the Equation (3). It is noted that T_s is the simulation time applied in this study. In reality, such a time can be the running time of the entire network.

$$J = IATE = \int_0^{T_s} \left(|\Delta f_1(t)| + |\Delta f_2(t)| + |\Delta P_{tie}(t)| \right).tdt \quad (3)$$

3. System Modelling under Study and Numerical Simulations

3.1. System Modelling

Figure 7 presents a block diagram of a fundamental power generation unit encompassing a governor, turbine, and generator. Turbines can be of various types, including but not limited to non-reheat, reheat, heat recovery, hydraulic, and gas turbines.

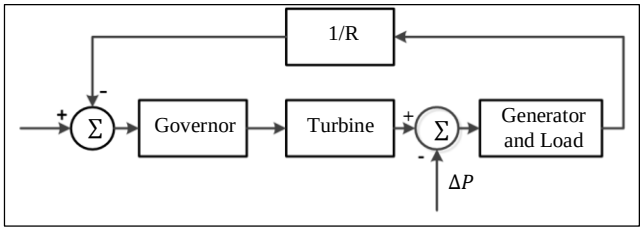

Fig. 7 A typical block diagram of an area in the electric power system

Transfer functions represent renewable energy sources in the following formulas:

$$\frac{\Delta P_{wtg}(s)}{\Delta P_{wt}(s)} = \frac{1}{T_{wts}s+1} \quad (5)$$

$$\frac{\Delta P_{spv}(s)}{\Delta P_{sp}(s)} = \frac{1}{T_{spv}s+1} \quad (6)$$

Where T_{wts} and T_{spv} are time constants.

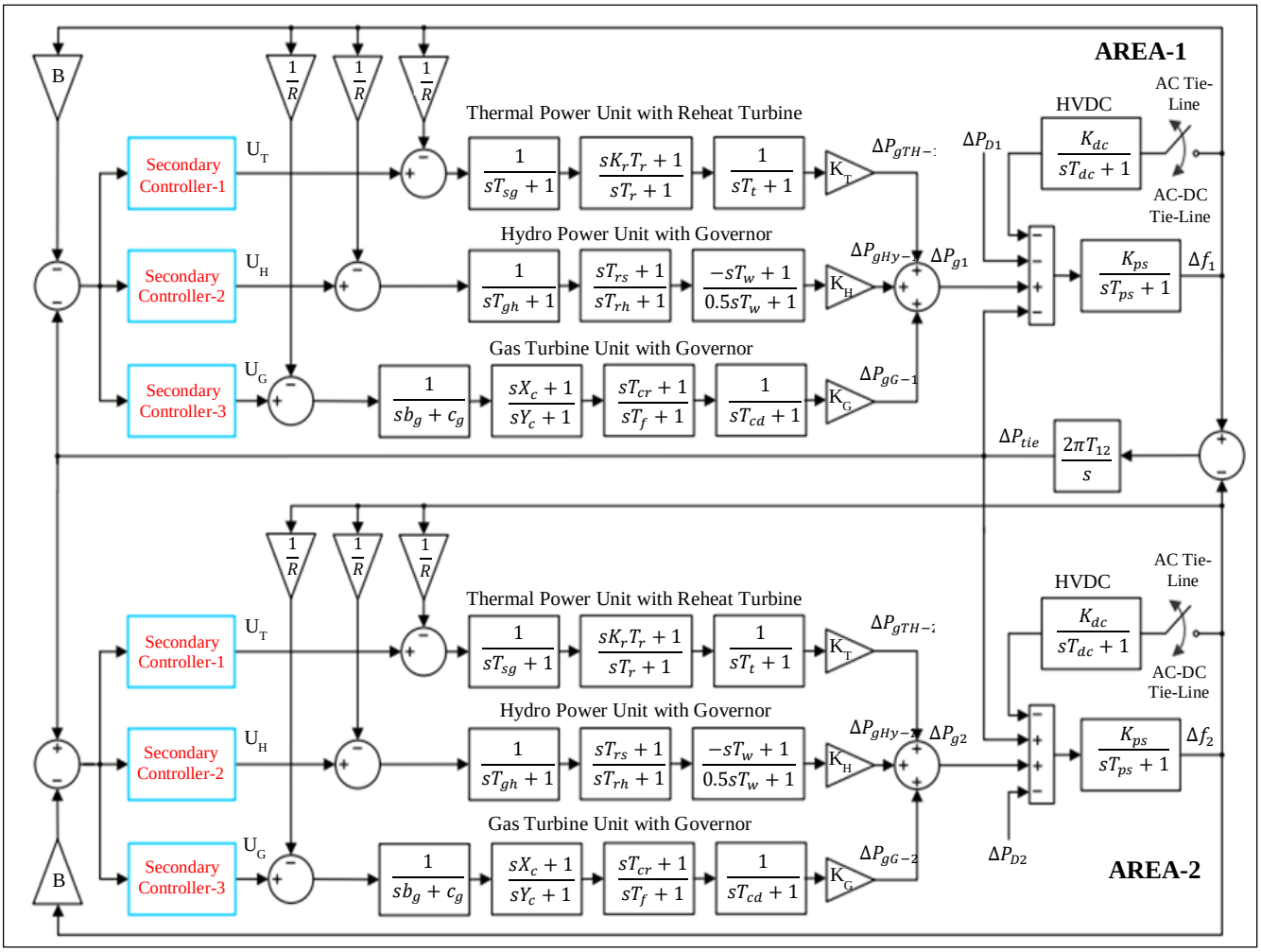

Fig. 8 The studied two-area power network model with HVDC and renewable resources established in MATLAB/Simulink

The power system considered in Figure 8 includes two areas, with each zone having 3 different turbines. The article considers renewable energy sources and HVDC, making the network more complicated and challenging. This is a more practical aspect to demonstrate the effectiveness of the proposed control methodology.

3.2. Numerical Simulations

To comprehensively evaluate the proposed controller's efficacy, the article presents simulations encompassing an expanded system model. This enhanced model incorporates the presence of Renewable Energy (RE) sources, High Voltage Direct Current (HVDC) transmission, and diverse load profiles characterized by varying shapes and magnitudes. The simulations explore the controller's performance under these various operating scenarios.

Case 1: All of the load changes are step types. $\Delta P_{D1} = 0.03$ (p.u.); $\Delta P_{D2} = 0.05$ (p.u.); $\Delta P_{spv} = 0.06$ (p.u.); $\Delta P_{wts} = 0.04$ (p.u.). Simulation results are illustrated in Figures 9(a) and (b) for both the deviations of frequency in two areas for all three controllers: the *i*PSO-based proposed controller, the traditional PSO-based PID counterpart and finally, the conventional PID one (tuned by the simulink tool in MATLAB).

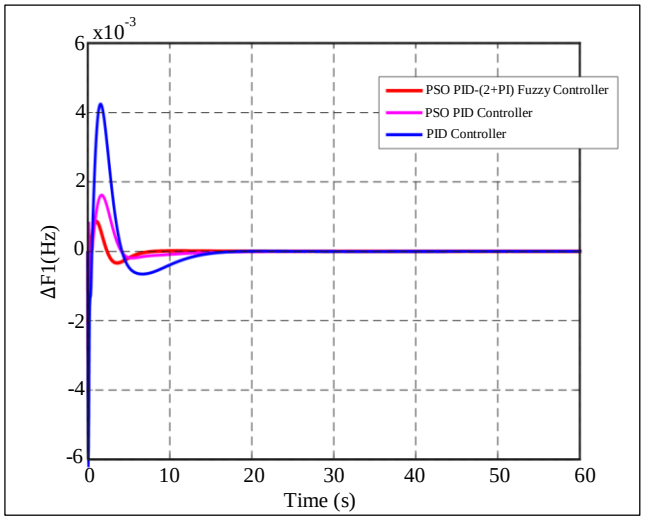

(a)

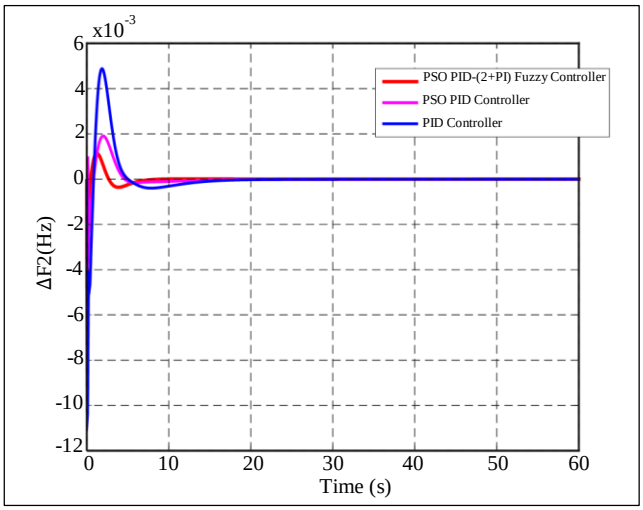

(b)

Fig. 9 Dynamic response frequency in three areas (in case 1) (a) ΔF1, and (b) ΔF2.

Case 2: ΔP_{D1} = 0.03 (p.u.) (Type of step); ΔP_{D2} = 0.03 (p.u.) (Type of random); ΔP_{spv} = 0.06 (p.u.); ΔP_{wts} = 0.05 (p.u.). (Type of step). Numerical simulation results are shown in Figures 10 (a) and (b).

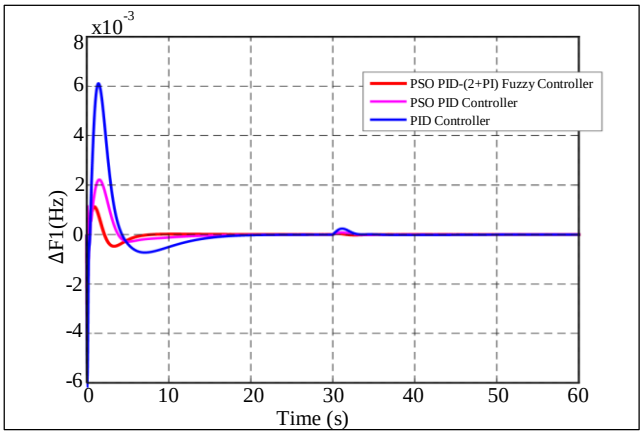

(a)

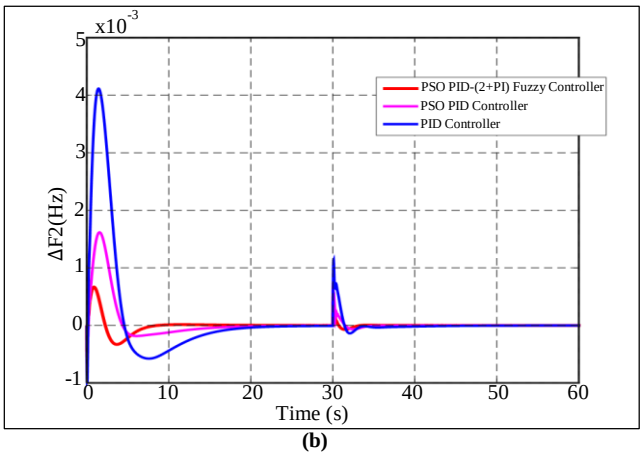

(b)

Fig. 10 Dynamic responses frequency in three areas (in Case 2) (a) ΔF1, and (b) ΔF2.

Case 3: ΔP_{D1} = 0.03 (p.u.) (Type of step); ΔP_{D2} = 0.03 (p.u.) (Type of pulse); ΔP_{spv} = 0.06 (p.u.); ΔP_{wts} = 0.03 (p.u.). (Type of step). Figures 11 (a) and (b) describe simulation results for this case.

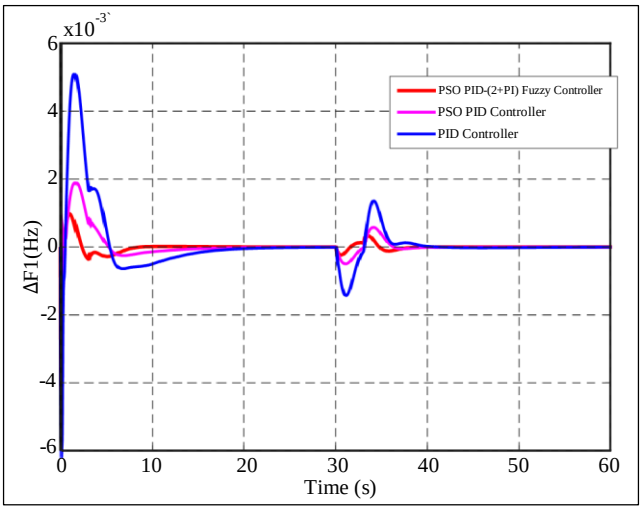

(a)

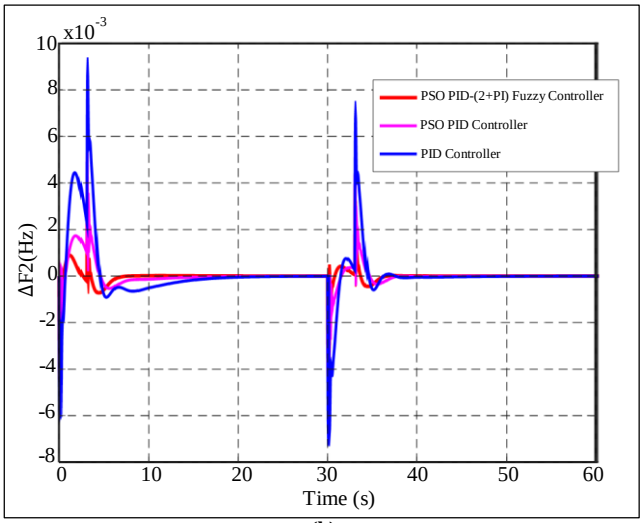

(b)

Fig. 11 Dynamic response frequency in two areas (in scenario 3) (a) ΔF1, and (b) ΔF2.

As illustrated in the simulation results presented in Figures 9 through 11, the proposed controller exhibits superior time response and overshoot performance compared to both the PSO-PID and conventional PID controllers. This advantage stems from the inherent simplicity of the PID controller, which unfortunately translates to slower response times and higher overshoot.

In contrast, the multi-stage controller, incorporating fuzzy logic and *i*PSO-optimized parameters, demonstrates a more effective response to frequency deviations within interconnected regions, particularly when accommodating the integration of renewable energy sources.

4. Conclusion and Future Work

The proposed controller demonstrably enhances the stability of the frequency error response in both areas compared to PSO-PID and conventional PID controllers. This improvement stems from the integration of two stages: a conventional PID regulator and a (2+PI) regulator, further augmented by a sophisticated fuzzy logic component. Additionally, the *i*PSO method, modified from the traditional PSO mechanism, facilitates the rapid identification of a suitable parameter set for effectively addressing the load-frequency control challenge within a large-scale multi-area electric power grid. Building upon this foundation, the current paper seeks to develop an even more effective optimal controller proposed to be applied in large-scale power networks, incorporating the complexities introduced by time delays and parameter uncertainties.

Acknowledgements

Electric Power University funds this research under research 2023, Project Granted number 2675-05/HĐ-ĐHĐL.

References

[1] E.S. Ali, and S.M. Abd-Elazim, "Bacteria Foraging Optimization Algorithm Based Load Frequency Controller for Interconnected Power System," *International Journal of Electrical Power & Energy Systems*, vol. 33, no. 3, pp. 633-638, 2011. [CrossRef] [Google Scholar] [Publisher Link]

[2] Sidhartha Panda, Banaja Mohanty, and P.K. Hota, "Hybrid BFOA-PSO Algorithm for Automatic Generation Control of Linear and Nonlinear Interconnected Power Systems," *Applied Soft Computing*, vol. 13, no. 12, pp. 4718-4730, 2013. [CrossRef] [Google Scholar] [Publisher Link]

[3] S.M. Abd-Elazim, and E.S. Ali, "Load Frequency Controller Design of a Two-Area System Composing of PV Grid and Thermal Generator via Firefly Algorithm," *Neural Computing and Applications*, vol. 30, pp. 607-616, 2018. [CrossRef] [Google Scholar] [Publisher Link]

[4] M. Farahani, S. Ganjefar, and M. Alizadeh, "PID Controller Adjustment Using Chaotic Optimisation Algorithm for Multi-Area Load Frequency Control," *IET Control Theory & Applications*, vol. 6, no. 13, pp. 1984-1992, 2012. [CrossRef] [Google Scholar] [Publisher Link]

[5] Gargi Konar, Kamal Krishna Mandal, and Niladri Chakraborty, "Two Area Load Frequency Control of Hybrid Power System Using Genetic Algorithm and Differential Evolution Tuned PID Controller in Deregulated Environment Transactions on Engineering Technologies," *Transactions on Engineering Technologies*, pp. 263-278, 2014. [CrossRef] [Google Scholar] [Publisher Link]

[6] Mahmoud Omar et al., "Optimal Tuning of PID Controllers for Hydrothermal Load Frequency Control Using Ant Colony Optimization," *International Journal on Electrical Engineering and Informatics*, vol. 5, no. 3, pp. 348-360, 2013. [CrossRef] [Google Scholar] [Publisher Link]

[7] Emre Çelik, "Improved Stochastic Fractal Search Algorithm and Modified Cost Function for Automatic Generation Control of Interconnected Electric Power Systems," *Engineering Applications of Artificial Intelligence*, vol. 88, 2020. [CrossRef] [Google Scholar] [Publisher Link]

[8] Mohamed A. Mohamed et al., "A Novel Adaptive Model Predictive Controller for Load Frequency Control of Power Systems Integrated with DFIG Wind Turbines," *Neural Computing and Applications*, vol. 32, pp. 7171-7181, 2020. [CrossRef] [Google Scholar] [Publisher Link]

[9] Binod Kumar Sahu, Swagat Pati, and Sidhartha Panda, "Hybrid Differential Evolution Particle Swarm Optimization Optimised Fuzzy Proportional-Integralderivative Controller for Automatic Generation Control of Interconnected Power System," *IET Generation, Transmission & Distribution*, vol. 8, no. 11, pp. 1789-1800, 2014. [CrossRef] [Google Scholar] [Publisher Link]

[10] Naglaa K. Bahgaat et al., "Load Frequency Control in Power System via Improving PID Controller Based on Particle Swarm Optimization and ANFIS Techniques," *International Journal of System Dynamics Applications*, vol. 3, no. 3, pp. 1-24, 2014. [CrossRef] [Google Scholar] [Publisher Link]

[11] Tarkeshwar Mahto, Hasmat Malik, and V. Mukherjee, "Fractional Order Control and Simulation of Wind-Biomass Isolated Hybrid Power System Using Particle Swarm Optimization," *Applications of Artificial Intelligence Techniques in Engineering*, pp. 277-287, 2018. [CrossRef] [Google Scholar] [Publisher Link]

[12] A.Y. Abdelaziz, and E.S. Ali, "Cuckoo Search Algorithm Based Load Frequency Controller Design for Nonlinear Interconnected Power System," *International Journal of Electrical Power & Energy Systems*, vol. 73, pp. 632-643, 2015. [CrossRef] [Google Scholar] [Publisher Link]

[13] S. Chaine, M. Tripathy, and Divesh Jain, "Non Dominated Cuckoo Search Algorithm Optimized Controllers to Improve the Frequency Regulation Characteristics of Wind Thermal Power System," *Engineering Science and Technology, An International Journal*, vol. 20, no. 3, pp. 1092-1105, 2017. [CrossRef] [Google Scholar] [Publisher Link]

[14] Meysam Gheisarnejad, "An Effective Hybrid Harmony Search and Cuckoo Optimization Algorithm Based Fuzzy PID Controller for Load Frequency Control," *Applied Soft Computing*, vol. 65, pp. 121-138, 2018. [CrossRef] [Google Scholar] [Publisher Link]

[15] E.S. Ali, and S.M. Abd-Elazim, "BFOA Based Design of PID Controller for Two Area Load Frequency Control with Nonlinearities," *International Journal of Electrical Power & Energy Systems*, vol. 51, pp. 224-231, 2013. [CrossRef] [Google Scholar] [Publisher Link]

[16] Emre Çelik et al., "(1 + PD)-PID Cascade Controller Design for Performance Betterment of Load Frequency Control in Diverse Electric Power Systems," *Neural Computing and Applications*, vol. 33, pp. 15433-15456, 2021. [CrossRef] [Google Scholar] [Publisher Link]

Appendix

f = 50 Hz, B = 0.4312 pu, R = 2.4 Hz/pu, Tsg = 0.08 s, Kr = 0.3, Tr =10 s, Tt = 0.3 s, Tgh = 0.2 s, Trs = 5 s, Trh =28.75 s, Tw = 1 s, bg = 0.05 s, cg =1, Xc= 0.6 s, Yc =1 s, Tcr = 0.01 s, Tf= 0.23 s, Tcd = 0.2 s, KT = 0.543478 pu, KH = 0.326084 pu, KG =0.130438 pu, T12 =0.0433, Kps =68.9566 Hz/pu MW, Tps =11.49 s, Kdc= 1, Tdc = 0.2 s.